

Partial spreading of a laser beam into a light sheet by shock waves and its use as a shock detection technique

J. Panda

University of Toledo, Toledo OH and

Resident Research Associate, NASA Lewis Research Center, Cleveland, OH 44135

Abstract

It is observed that, when a laser beam is allowed to fall on a shock surface at a grazing incidence, a small part of the beam spreads out in a thin, diverging sheet of light normal to the surface, and both upstream and downstream of the shock. The phenomenon is visualized by observing a cross section of the light sheet on a screen placed normal to the laser path after it touches a shock. The light sheet disappears when the beam is moved to any other locations where there is no shock or the beam pierces the shock surface, i.e., at a non-grazing incidence. The spread angle of the light sheet is considerably higher than the angle by which the beam may bend as it passes through the shock, which produces a small difference of refractive index. Various details indicate that the spread light is a result of diffraction of a small part of the laser beam by the shock whose thickness is nearly the same as that of the laser wavelength. Shocks formed in underexpanded free jets of fully expanded Mach numbers 1.4 to 1.8 are used for this experiment.

The above optical phenomenon is used as the basis of a novel shock detection technique which depends on sensing the spread light using a photomultiplier tube (PMT). The locations of the shock surfaces in the underexpanded supersonic jet, obtained using this technique, match with those inferred from the Schlieren photographs and velocity measurements. Moreover, if the shock oscillates, a periodic PMT signal is obtained which provides information about the frequency and amplitude of shock motion.

I. INTRODUCTION

The present paper describes a newly observed optical phenomenon that arises when a laser beam touches the surface of discontinuity produced by a shock, and a shock detection technique based on this phenomenon. Shocks formed inside underexpanded supersonic jets are used to demonstrate the optical phenomenon as well as to validate the shock detection technique. First, a brief description of the optical phenomenon is presented.

It is observed that, when a laser beam is allowed to become tangent to a shock surface, a small part of light from the beam diverges out in a thin sheet from the point of interaction. Figure 1 shows a schematic of this phenomenon. A conical shock surface is considered in this figure. A laser beam is moved to three different axial locations parallel to the axis of the cone. It is shown that a light sheet appears at location B, where the beam is tangent (i.e., at a grazing incidence) to the shock surface. When the beam is moved to the location C, where it pierces the shock surface, i.e., at an incidence angle other than the grazing one, the spread light disappears. The curvature of the shock surface is not responsible for the optical phenomenon, since, an interaction with a normal shock produces the same effect.

Possible physical reasons behind this optical phenomenon are discussed in the text. It is shown that the simple bending of the laser beam across the small difference in the refractive index produced across a shock is too small to be detected in this experiment and is incapable of explaining the observed phenomenon. Deflection of a laser beam while crossing a shock has been calculated (Kriksunov and Pliev¹) and measured (Faris and Byer²) following the Paraxial ray equation (Casperson³, Born and Wolf⁴). The angular deflection of the beam has been found to be very small, typically fraction of a degree; while the spread angle (θ) of the light sheet associated with the present optical phenomenon is large, between 10° to 25° depending on the shock strength.

Propagation of electromagnetic waves through a medium of varying refractive index, such as that produced

by a random turbulent field, is a classical problem and has been addressed by many researchers, e.g., Tatarskii⁵ and Clifford⁶. In all such analysis a fundamental assumption is a slow spatial variation of the refractive index such that the gradient is negligible. Across a shock, the absolute change of refractive index is small, but the gradient is very high as the change occurs over the shock thickness which is as short as the optical wavelength. Therefore, the above analyses are inadequate to explain the observed shock-laser interaction phenomenon. Various details observed in the visualization photographs indicate that a part of the laser beam might have been diffracted by the shock wave. The reasoning leading to this conclusion are discussed following a presentation of the photographic evidences.

Traditionally, all shock detection techniques, e.g., Schlieren (Merzkirch⁷), Shadowgraph (Sajben and Crites⁸) and Tomography (Faris and Byer²), are based on the principle of simple deflection of a light ray while crossing the refractive index difference produced across a shock. The detection technique presented in this paper, on the other hand, depends on the diffraction phenomenon as described earlier. A simple arrangement is made in which the appearance of the light sheet is sensed using a photomultiplier tube (PMT). When a shock containing flow field is scanned by a laser beam, a non-zero voltage output from the PMT circuit is obtained only when the beam is tangential to the shock surface. The technique was validated in the shock containing plumes of supersonic underexpanded jets, by comparing the shock locations identified by the present optical technique, Schlieren photography and a limited Laser Doppler Velocimetry measurement of the jet centerline velocity. Excellent agreement is found in the shock locations identified by all of these methods. In addition it is shown that the present method is able to provide the frequency and amplitude of the oscillating shock waves. The formation and the passage of the organized, turbulent structures in the shear layer of free, supersonic jets make the shocks unsteady and also produce intense screech tones and broadband noise (Tam⁹, Norum and Seiner¹⁰). Shocks are found to oscillate at the screech frequency. A detailed account and a comparison of this technique to the Schlieren method are presented in the later portion of section III.

II. EXPERIMENTAL SET-UP

Jet facility: A schematic of the jet facility used for this experiment is shown in figure 2. Compressed, dry (dew point = -68°C) air at room temperature is supplied at the left into the 203 mm diameter plenum. The air successively flows through perforated plates, an acoustically treated section (to reduce the upstream valve and entrance noise), a turbulence management section containing a set of coarse and fine screens and an area contraction of 64 before discharging into the ambient air through a 25.4 mm diameter convergent nozzle. There is a provision to inject seed particles in the plenum for LDV measurements. The fully expanded Mach numbers of the underexpanded supersonic jets used in the present experiment were in the range 1.2 to 1.8. The jet Mach number was varied by changing the supply pressure to the plenum through a set of remote-controlled and manually operated valves. The noise characteristics of the jets were measured by a microphone, mounted at the nozzle lip, facing the downstream direction.

Schlieren system: A standard Schlieren system using two 100 mm diameter spherical mirrors was used to visualize the shock containing plume. The knife edge position was vertical; therefore, the horizontal density gradient is visible in all the photographs presented in this paper. Light from the knife edge was allowed to fall directly on a Nikon F4 camera which permitted a maximum shutter speed of 1/8000th of a second. Photographs taken with a steady light as well as with a single spark are presented in this paper. Since the Schlieren system permitted viewing only a relatively small axial distance (less than four jet diameters), the whole system was moved to different downstream locations to be able to visualize a longer extent of the flow field.

Laser Doppler Velocimetry (LDV): Only a limited amount of time averaged axial velocity data obtained from a 1-component, dual-beam, and forward scatter, LDV system will be presented in this paper. The LDV system consists of a 4-Watt, Lexel, Argon-ion Laser as the light source, a TSI Colorburst unit (TSI 9201) for color separation and beam splitting purposes, fiber-optic cables and a two-component fiber optic probe (TSI 9118). To minimize the particle lag in the shock containing plume, very small diameter (0.6 μm) polystyrene latex (PSL) spheres were used

as seed particles. The Doppler burst frequency was measured by a TSI 1990C signal processor. The LDV system had a fringe spacing of 3.6 μm , with a probe volume diameter of 0.16 mm and length of 1.7 mm. The Doppler frequency from the supersonic jet flow was very high and frequently overshoot the measurable limit of about 150 MHz of the TSI counters. To overcome this difficulty, a 40 MHz frequency shift was used. The fringes were continuously moved along the direction of the flow; thereby reducing the effective Doppler shift frequency. Only time averaged velocity measurements are presented in this paper.

III. RESULTS AND DISCUSSION

The optical phenomenon and the shock detection technique were studied in the underexpanded supersonic jets generated from the facility shown in figure 2. The flow field of such a jet contains quasi-periodic shock cell structures which are formed as the jet adjusts to the difference between the nozzle exit pressure and the ambient pressure (Shapiro¹¹). Each shock cell contains an expansion region through which the jet velocity increases, and an oblique or normal shock (Mach disk) across which the jet velocity drops suddenly. The optical phenomenon of interest is demonstrated as the result of an interaction between a laser beam and the first shock surface formed in such jets. The light sheet, which diverges away from the main beam from the point of interaction, is studied by placing a semi-transparent screen normal to the beam path. In the following, details of the optical set-up, visualization photographs, and possible physical reasons behind this phenomenon are discussed first. The shock detection technique is discussed next. In many ways the technique is superior to the conventional Schlieren method in detecting the location and unsteadiness of shocks. Measurement of shock unsteadiness and relative merits of the present method over the Schlieren method are discussed at the end of this section.

A. Optical Phenomenon: Visualization

The laser beam, used for studying the light spreading phenomenon, is a part of the fiber-optic, Laser Doppler Velocimetry (LDV) system described earlier. However, to study the light spreading phenomenon, only one of the beams (green, 0.514 μm wavelength) was used and the rest were blocked. The diameter of the beam out of the optical fiber is about 2 mm which is then focused at the jet centerline to a diameter of 0.16 mm.

Figure 3 shows a schematic of the visualization set-up. The laser beam, after passing through the jet flow field normal to its axis, is allowed to fall on a semi-transparent screen. The screen is made of a piece of semi-transparent graph paper whose optical behavior is similar to a ground glass. It was mounted parallel to, and 280 mm away from the jet axis. Therefore, a normal cross-section of the light sheet was visible on the screen. It was found that the relatively weak light from the spread portion of the beam became completely overwhelmed by the intense main beam if the latter was allowed to fall directly on the screen. Therefore, a small, 4.8 mm diameter hole was made in the screen to allow the main beam to go through. The light pattern on the semi-transparent screen was photographed by a 35 mm Nikon F4 camera and are presented in the next two figures. The optical set-up (fiber-optic probe, screen and the beam stop; figure 3) was mounted on a 3-axis Klinger traversing unit which allowed it to be moved along the stream-wise and the transverse directions.

For the photographs, demonstrating the laser shock interaction, the first shock surface formed inside underexpanded jets is used. This shock is relatively steady and can be of different shape. Flow direction in all photographs is from left to right, and the laser power used is low: 50 to 100 mW. To identify and visualize the shock surfaces, Schlieren photographs of the jet flow fields are also presented. A fast shutter speed of 1/4000 second is used for the Schlieren photographs while a slow shutter speed of 1/15 to 1/8 second is used for the laser light photographs.

Figure 4(a) shows a Schlieren photograph of the underexpanded jet at a fully-expanded Mach number 1.4. The 2-dimensional projection of the shock surfaces visible in this photograph is triangular, indicating conical surfaces in the actual axisymmetric flow field. The apex of the cone is at the centerline of the jet and the base is formed along the outer periphery containing the shear layer. Of the two shock surfaces seen in figure 4(a), the first surface oscillates by a considerably smaller amplitude (less than 2 mm, as discussed later in the text) and therefore, has a more definite boundary. A small measuring scale of 25.4 mm length, kept in the field of view to provide a

measure of distance, is visible at the bottom of the Schlieren picture.

Figure 4(b) shows the locations of the laser beam with respect to the first shock surface for the photographs of figure 4(c). The photographs presented in figure 4(c) are normal cross sections of the light sheet as sketched in the front view of figure 1. As discussed earlier, the hole, appearing as a dark spot, allows the main laser beam to pass through. In photograph I (figure 4c), the laser beam is upstream of the shock and any unusual optical phenomenon is absent. The low level of background illumination on the screen is caused by the reflected light from the lens surfaces of the fiber-optic probe. In photographs II and III the beam is grazing the shock surface at $z/D = -0.45$ and 0.3 , respectively. Cross-sections of the light sheet in each of these photographs appear as two bright rays of light spreading out from the main laser beam in both upstream and downstream directions normal to the shock surfaces. Notably, the directions of the light spread are also the direction of local refractive index gradients produced due to the density difference across the shock. Upon further visual inspections, it is found that the light sheet is diverging from the laser beam from a location where the beam touches the shock surface. The divergence angle, θ , of the light sheet, calculated from photograph II is about 10° (noting that the screen is placed 280 mm away from the jet axis). The total energy in the light sheet is a small fraction (between 2% to 4%) of that of the main beam. Both the intensity and the divergence angle of the light sheet increase as the shock strength is increased. The light sheet is somewhat brighter in the downstream, higher refractive index side of the shock (this difference can be seen clearly in the photographs presented in the next figure).

Photograph IV (figure 4c) shows weaker spreading of the beam when it passes through the base of the shock cone. In this region the shock surface terminates in the shear layer; the shock pattern is complex and the shock strength is diminished. It should be noted that, for the present set-up, the light sheet appears only when the laser beam is placed along the triangular, outer trace of the shock surface shown in figure 4(a). Along this trace, the laser beam is at a grazing incidence to the shock surface. At any other locations where there are no shocks or the beam pierces through the conical shock surface, i.e., at a non-grazing incidence, the photograph of the screen is similar to that of I (figure 4c).

Figure 5 shows photographs similar to those of figure 4, but for a fully expanded Mach number of 1.8. The appearance of the first shock surface is very different; a Mach disk has formed, the barrel shock from the nozzle lip to the Mach disk is clearer, and there is a reflected shock from the tip of the Mach disk to the shear layer around the jet (Adamson and Nicholls¹²). The Mach disk is equivalent to a normal shock across which the jet velocity drops from supersonic to subsonic Mach numbers. In three dimensions the Mach disk and the reflected shock appear as a truncated cone. Each photograph of figure 5(b) shows a few faint lines corresponding to the shock boundary. These lines are formed as a result of the shadowgraph image of the first shock cell on the screen produced by the low level, background illumination.

Photographs I, II and III of figure 5(b) were obtained by traversing the laser beam in the axial direction, across the Mach disk. For the latter two photographs, the laser beam was moved downstream by, respectively, 0.3 mm and 0.6 mm from its position in photograph I. At location I the beam just touches the upstream side of the Mach disk. The pattern on the screen shows definite secondary maxima in the light intensity distribution on both sides of the shock. Visual investigation revealed one more maximum further to the right beyond the width of the screen. The angular distance between the main beam and each of the secondary maxima, estimated from photograph I of figure 5(b), is quite large, about 12.5° . As the beam is moved further downstream, very slowly through the shock, the secondary maxima come closer to the beam forming a continuous light sheet. In photograph II the divergence angle of the light sheet is still very high, about 20° . It is believed that, in this photograph, the Mach disk is nearly at the center of the beam cross-section and in III it is to the left, but still touching a portion of the beam. In the latter photograph, the light ray on the upstream side of the shock is very weak indicating a dimmer light sheet. In photograph IV the beam was moved to a position where all three shock surfaces (the barrel shock, the Mach disk and the reflecting shock) merge. As expected, the photograph indicates light sheets formed along directions normal to each of the shock surface.

The spread light pattern is found to be independent of the polarization of the laser beam. This was observed by changing polarization of the incident beam through a polarization rotator placed in front of the fiber-optic probe.

The light sheet was also visible when the blue beam (wavelength = .488 μm) instead of the green (.514 μm) was used.

B. Discussion of possible physical reasons:

The optical phenomenon can not be described as light scattering from small particles since, the basic pattern and directivity of the light sheet is uncharacteristic of scattered light from small particles. Moreover, clean and dry air of dew point of -68°C was used; this eliminates the possibility of significant condensation in the flow.

A light beam is deflected from its original path as it passes through the shock. However, the deflection of the primary beam was so small that it always passed through the 4.8 mm hole made on the screen. Another relevant concern is the effect of shock unsteadiness. The first shock was oscillating by less than ± 1 mm (to be shown later) about its mean position. However, the resulting oscillation of the laser beam was too small to be detected, as the beam passed through the central hole on the screen independent of the appearance or disappearance of the light sheet. It should be emphasized here that the light pattern observed on the screen is not due to any deflection of the laser beam, but is a result of spreading of a small fraction of light from the main beam. A farther analysis of the associated flow and optical parameters and the inapplicability of the Geometrical Optics to explain the observed phenomenon are discussed in the following.

A significant change of pressure, temperature and density of the gas across a shock wave is accompanied by a change in the refractive index. Upstream of the shock is a region of lower refractive index and downstream is a region of higher refractive index. For the Mach disk of $M_j = 1.8$ jet (which corresponds to the photographs of figure 5) various parameters are estimated and are shown in Table I. The Mach number upstream of the Mach disk is obtained from the solution of the axial velocity distribution along the centerline of an axisymmetric jet by Owen and Thornhill¹³. The solution is valid up to the first shock surface formed in underexpanded jets from a sonic nozzle (Adamson and Nicholls¹²). The downstream Mach number is obtained by using normal shock relations. The static pressure and air density are calculated using isentropic relations from the known total pressure and total temperature. After knowing the air density, the refractive indices upstream and downstream of the Mach disk are calculated using the Gladstone-Dale formula; $(n-1)=k\rho$, k =Gladstone-Dale constant (Merzkirch⁷). From various earlier measurements and analytical solution of the Navier-Stokes equations it is known that the thickness of the normal shock varies between 3 to 5 molecular free paths (see Cowan and Hornig¹⁴, Sherman¹⁵), which is calculated from the estimated upstream static pressure and temperature (Smithsonian Physical Table¹⁶).

As mentioned earlier, the change in the refractive index even across the Mach disk, as shown in Table I, is small. The beam steering effect due to refraction of light across the shock is also expected to be small. The analyses of Kriksunov and Pliev¹ and Faris and Byer² of deflection of light across a shock, based on the paraxial ray equation, show that the expected deflection angle is only a fraction of a degree, while the measured spread angle of the light sheet is between 10° and 25° . The phenomenon appears when the laser beam is tangential to the shock surface. In this condition the thickness of the shock plays an important role. The situation is shown in Figure 6. A cross-section of the beam is seen in this figure. The shock represents an interface, along the direction of beam propagation, separating two homogeneous media. As shown in Table I, the thickness of this interface is nearly the same as that of the light wavelength. In this situation the fundamental approximation of the Geometrical Optics, i.e., the length scale over which any change of optical property may occur is much longer than the wavelength of the light (Born and Wolf⁴), is violated. Therefore, calculations based on the rules of geometrical optics such as the paraxial ray equation becomes invalid and cannot account for the observed phenomenon. Another evidence demonstrating the failure of the Geometrical Optics is the upstream part of the light sheet. Nearly half of the spread light appears upstream of the shock which is *opposite* to the direction of the gradient of refractive index created across a shock. Yet, according to the laws of the Geometrical Optics, the laser beam is expected to bend only *along* the direction of refractive index gradient.

Diffraction of the laser beam is naturally expected in such a situation. Possibly, a part of the beam around the thin shock is diffracted forming the diverging light sheet whose cross-section is visible in Figs. 4 and 5. The secondary maxima visible in photograph I of figure 5(b) supports this argument. The present optical phenomenon

should also appear in Schlieren and Shadowgraph images of shock containing flow fields. However, in these techniques the illuminance (luminous intensity per unit area) around the shock is far less than that of the laser beam used for the present experiment. Therefore, the faint diffracted light becomes undetectable in the final image.

The observed optical phenomenon is a challenging problem in any account, and further study is needed for a better understanding of this problem.

C. Shock Detection Technique:

The optical phenomenon, described above, is conveniently used as the basis of a unique shock detection technique. It depends on scanning a shock containing flow field with a laser beam and sensing the presence of the spread light using a photomultiplier tube (PMT). The incident beam locations which correspond to the non-zero PMT signal are the shock locations.

Figure 7 shows a schematic of the set-up which is similar to that used for the visualization purpose except for the light collecting and sensing devices that replace the screen. Just in front of the 60 mm diameter collecting lens is a 13 mm diameter beam stop which blocks the main beam from entering the collecting optics. However, the diameter of the beam stop is small enough to allow most of the spread light from the diverging light sheet to enter the collecting optics. The collecting lens focuses this light to a 0.2 mm diameter pinhole which then passes it to a photomultiplier tube (PMT, TSI model 9162). The electrical output from the PMT is connected across a 50 Ohm terminator (not shown in figure 7). The voltage drop across the terminator is proportional to the PMT current and, therefore, is an indicator of the intensity of the collected light. As with the visualization arrangement, the complete optical set-up was mounted on a 3-axis Klinger traversing unit which allowed it to be moved along the stream-wise and the transverse directions within accuracy of .025 mm. Under normal circumstances no light from the laser beam reaches the PMT. However, if the optical arrangement is moved to a location where the laser beam touches a shock surface, a part of the spread light is collected and sensed by the PMT which then produces a non-zero output. The analogue voltage signals from the PMT, as well as the microphone outputs, were digitized using a dsp Technology sample-and-hold digital converter and then stored and processed by MicroVAX 3300 computer.

Figure 8 shows the voltage-time traces obtained from the PMT when the laser beam was placed at three closely spaced axial stations near the apex of the first shock surface in the $M_j = 1.4$ jet. Figure 8(b) was obtained when the beam touched the shock surface. Figures 8(a) and 8(c) correspond to locations, respectively, 2.5 mm upstream and 2.5 mm downstream from that of figure 8(b). In the former, there is no shock wave in the path of the laser beam and in the latter the beam pierces the shock surface. In both of these situations PMT signal was nearly zero as no light was collected. The nearly periodic negative spikes of figure 8(b) indicate that the optical phenomenon appears and disappears periodically as the oscillating shock moves in and out of the laser beam. The amplitude of shock oscillation was nearly $\pm 1^\circ$. This will be discussed later in the text.

The availability of an electrical signal, similar to that of figure 8(b), which is indicative of a shock surface touching the laser path, is the basis of the detection technique. Usually, the root-mean-square (rms) value of the voltage drop across the PMT is measured as the optical arrangement is traversed from point to point in the flow field. Whenever the beam grazes a shock surface the rms of the PMT voltage jumps from a near zero to a large value. As a shock containing flow field is scanned by the laser beam, locations from where a non-zero PMT signal is obtained, correspond to points on the shock surface.

D. Validation of the technique:

The shock surfaces identified in an underexpanded jet of $M_j = 1.4$ by this technique are compared with those inferred from the Schlieren photographs, and LDV measurements of the velocity distribution. Data obtained by laser surveys and a spark-Schlieren photograph of the first shock cell of an $M_j = 1.4$ jet are shown in figure 9. The markers seen at the bottom of figure 9(a) are placed one jet nozzle diameter apart. The rms value of the voltage drop across the PMT, obtained as the flow field is surveyed at three radial locations, are shown in figures 9(b), (c) and (d). At $z/D=0.45$ (close to the shear layer) the Schlieren photograph indicates the presence of the shock surface at about $x/D = 1.2$. The laser survey (figure 9b) also indicates a large rms voltage around the same axial position. At the other two

radial locations, centerline and $z/D = 0.2$, the light sheet is expected to appear twice. First, when it touches the conical shock boundary and second when it touches the base of the cone. As mentioned earlier, at the latter location the shock splits into many 'legs' as it ends in the shear layer and any one of these 'legs' can be tangential to the laser beam. The laser surveys of figure 9(c) and (d) show large rms voltages exactly around these expected locations as identified from the Schlieren photograph. The third spike in the centerline survey (figure 9d) is possibly due to another shock-like discontinuity seen further downstream of the first shock in the Schlieren photograph.

The data shown in figure 9 are in the vicinity of the first shock cell only. The spark Schlieren photographs, laser survey and the Mach number distribution along the centerline covering all shocks formed in $M_j = 1.4$ jet are shown in figure 10. For Schlieren visualization, mirrors had to be placed at two different axial positions to cover the desired downstream distance. Therefore, the two photographs of figure 10(a) were taken at different instances and the knife edge cut-off was also different between them. A marker, consisting of long tubes kept one nozzle diameter apart, was placed parallel to the jet axis as an indicator of the downstream distance. It is also used to match the two photographs. The spark duration time ($>60 \mu s$) was too long to freeze the motion of the turbulent eddies, yet it was sufficient to stop the motion of the shocks which move by a relatively smaller amplitude. The first shock surface was the steadiest and had the best defined boundary. The shock formed further downstream became increasingly distorted. Unlike the conical appearance of its predecessors the fourth surface appears almost like a disk.

The centerline laser survey of figure 10(b) is characterized by quasi-periodic regions of high and nearly zero rms voltages. As mentioned earlier, axial locations of high PMT voltage correspond to the shock positions. Data up to $x/D = 1.5$ are the same as presented in figure 9(d). However, a different scale used for the abscissa causes the difference in the appearance. Good agreement can be seen between the shock positions identified in the laser survey (figure 10b) and those seen along the centerline of the Schlieren photograph (figure 10a). The origin of the distinct spikes around the first shock surface is explained earlier. However, the variation of the rms voltage around the subsequent shocks is difficult to explain. It is believed that the large turbulent structures, present in such jets, progressively distort the shocks formed further downstream. However, further studies are necessary to understand the unsteadiness of different shocks formed inside underexpanded jets.

Figure 10(c) shows the centerline Mach number distribution obtained from the LDV measurements of the time averaged axial component of velocity. The purpose of the LDV data is to identify the shock locations. Therefore, measurement inaccuracies due to particle lag will not be discussed here. The Mach number distribution, calculated from the time averaged axial velocity measurements, shows many undulations with the local value overshooting the fully expanded jet Mach number and then dropping close to unity. The regions over which the local Mach number increases correspond to the expansion regions of the jet and the axial stations where the Mach number starts to drop can be considered as the shock locations. The shock locations indicated from the LDV data match with the corresponding locations indicated by the laser survey. This reconfirms the usefulness of the present optical technique in identifying the shock locations.

E. Measurement of shock unsteadiness

It has been shown in figure 8(b) that an unsteady PMT signal is obtained when the laser beam is positioned to touch an oscillatory shock. A spectral analysis of the unsteady PMT signal provides the frequency of shock oscillation. Figure 11 shows a comparison between an acoustic spectrum measured using a microphone and spectra of the shock motion obtained from the PMT signal. The microphone was placed at the nozzle lip (see figure 2) to monitor the jet noise. Peaks, seen in the narrow-band noise spectrum of the $M_j = 1.4$ jet (figure 11a), correspond to the screech frequency (5.5 kHz) and a few of its harmonics. Figure 11(b) presents two spectra of the PMT signal when the laser beam was positioned on the first two shock surfaces individually. Both spectra show distinct peaks at the fundamental and harmonic of the screech frequency, which indicates that both shocks oscillate primarily at the screech frequency. This observation is supported by an earlier experiment of Lessiter and Hubbard¹⁷ who photographed shadowgraph images of the jet using high speed movie camera to determine the frequency of shock motion.

The amplitude of shock oscillation can also be determined by using the present shock detection technique.

This is best demonstrated through figure 9, where data from laser survey around the first shock surface is presented. For every encounter with the shock surface, a high value of the PMT signal is obtained over an axial extent through which the shock oscillates. This is seen as the width of the high rms regions in figures 9(b), (c) and (d). The average width is measured to be $0.67d$ (1.7 mm), which represents the amplitude of oscillation of the first shock surface. The measurement is accurate within the laser beam diameter, 0.16 mm for the present case.

F. Comparison with Schlieren and shadowgraph methods.

As a shock detection technique, there are a few definite advantages of the present optical method over the Schlieren or the shadowgraph methods. First, both of the latter two methods depend on the density fluctuations in the flow field. Such density changes can be caused by various sources, such as random turbulent fluctuations, variation of concentration of different species as well as by shock waves. In principle, neither the Schlieren nor the Shadowgraph method can differentiate the density changes only due to the shock wave from the other sources. The problem becomes especially acute if one tries to obtain quantitative data from Schlieren images using a light sensing device (Powell¹⁸). The present optical technique, on the other hand, depends on a sharp density change over a very small distance, found only in the shock waves. Therefore, properties of the shock surfaces can be measured without any ambiguity using this technique.

The second advantage of the current method lies in its simplicity and accessibility. The large Schlieren mirrors and the other accessories are difficult to use in complex flow geometry, such as a turbo machinery flow passage. However, the current method depends on a thin laser beam that is far more accessible and can be used much more conveniently in complex geometries.

The present optical technique is non-intrusive and is useful for a point by point survey to provide quantitative information about the exact locations and unsteadiness of shocks. However, it does not provide a global view of the flow field for which Schlieren or shadowgraph methods are still necessary.

IV. CONCLUSION

The present paper reports an optical phenomenon, and a shock detection technique based on this phenomenon. The former is visualized as the appearance of a thin sheet of light diverging from a laser beam which is incident at a grazing angle on a shock surface. The principle features of the optical phenomenon are summarized as follows:

(a) This phenomenon appears only when the laser beam grazes a shock surface. It completely disappears at any other incidence.

(b) The divergence angle of the light sheet is very high, between 10° to 25° depending upon the shock strength.

(c) The spread light is visible both upstream and downstream of the shock along the direction of the local gradient of the refractive index.

(d) When the laser beam interacts with a strong normal shock, produced as a Mach disk in an underexpanded free jet, secondary maxima similar to those observed in a line diffraction pattern are observed.

(e) The spread light is not affected by any change of polarization of the laser beam.

Scattering from small particles cannot be the source of this spread light. Also a simple analysis, based on the deflection of the laser beam caused by the small change in refractive index cannot explain this phenomenon. Since the shock thickness is nearly the same as the wavelength of the laser light used, it is argued that a steep gradient in the refractive index within such a short distance may have diffracted a part of the laser beam. The problem is a challenging one and further research is necessary to explain this phenomenon.

This optical phenomenon is conveniently used as the basis of a novel shock detection technique to identify the location of a shock and to quantify its unsteady motion. The technique is based on sensing light that falls far away from the main laser beam as it touches a shock surface. Excellent agreement is found in the shock locations identified by this technique and those identified through Schlieren photography and velocity measurements. As a demonstration of the usefulness of this technique in measuring shock unsteadiness, frequency and amplitude of the oscillating shocks in underexpanded free jets are also measured. The frequency is found to be the same as that of the

screech tone emitted by the jet.

ACKNOWLEDGEMENT

The author wishes to acknowledge the help of Dr. R. M. Chriss and Dr. A. J. Strazisar in setting up the LDV unit. He also acknowledges the helpful discussions with Mr. G. Adamovsky, Dr. R. G. Seasholtz, Dr. K. B. M. Q. Zaman and Dr. G. Raman on the optical phenomenon and shock oscillation.

Reference

- ¹Kriksunov, L. Z. and Pliev, A. E. "Refraction of laser beams at a compression shock," Sov. J. Opt. Technology, Vol. 51, No. 7, (July 1984); English Translation by the Optical Soc. of America (1985).
- ²Faris, G. W. and Byer, R. L., "Three-dimensional beam-deflection tomography of a supersonic jet," Applied Optics, Vol. 27, No. 24, pp. 5202-5212, (Dec. 1988).
- ³Casperson, Lee, W., "Gaussian Light Beams in Inhomogeneous Media," Applied Optics, Vol. 12, No. 10, pp. 2434-2441, (1973).
- ⁴Born, M. and Wolf, E., "*Principles of Optics*," Sixth edition, Pergamon Press, (1989).
- ⁵Tatarski, V. I., "*Wave Propagation in a Turbulent Medium*," Translated from the Russian by R. A. Silverman, McGraw-Hill Book Co., Inc., (1961).
- ⁶Clifford, S. F., "The Classical Theory of Wave Propagation in a Turbulent Medium," Topics in Applied Physics, Vol. 25, "*Laser beam propagation in the atmosphere*," Ed. J. W. Strohbehn, Springer-Verlag, (1978).
- ⁷Merzkirch, W., "*Flow Visualization*," Academic Press (1987).
- ⁸Sajben, M. and Crites, R. C., "Real-Time Optical Measurement of Time-Dependent Shock Position," AIAA J., Vol. 17, No. 8, pp. 910-912, (Aug. 1979).
- ⁹Tam, C. K. W., "Jet Noise Generated by Large-Scale Coherent Motion," NASA RP 1258, Aerodynamics of flight vehicles: Theory and Practice, Vol. 1 Noise sources (1991).
- ¹⁰Norum, T.D. and Seiner, J. M., " Location and Propagation of Shock Associated Noise from Supersonic Jets," AIAA 80-0983, (1980).
- ¹¹Shapiro, A. H. "*The Dynamics and Thermodynamics of Compressible Flow*," (1953).
- ¹²Adamson, T. C. and Nicholls, J. A., "On the Structures of Jets From Highly Underexpanded Nozzles Into Still Air," Journal of the Aero/space Sciences, pp. 16-24, Jan. (1959).
- ¹³Owen, P. L. and Thornhill C. K., "The Flow in an Axially-Symmetric Supersonic Jet from a Nearly-Sonic Orifice into a Vacuum," A.R.C. Technical report, R. & M. No. 2616, (1952).
- ¹⁴Cowan, G. R. and Hornig, D. F., "The Experimental Determination of the Thickness of a shock front in a gas," J. Chem. Phys., Vol 18, pp 1008-1017 (1950).
- ¹⁵Sherman, F. S., "A Low-Density Wind-Tunnel Study of Shock-Wave Structure and Relaxation Phenomenon in Gases," NACA TN3298, (1955).
- ¹⁶*Smithsonian Physical Tables*, prepared by W. E. Forsythe, published by the Smithsonian Institute, (1956).
- ¹⁷Lassiter, L. W. and Hubbard, H. H., "The Near Noise Field of Static Jets and Some Model Studies of Devices for Noise Reduction," NACA TN 3187, July (1954).
- ¹⁸Powell, A., "On The Mechanism of Choked Jet Noise," Proc. phys. Soc. (London), Vol. 66, pt. 12, No. 408B, pp. 1039-1056 (1953).

Table I. Estimated values of parameters relevant to the optical phenomenon observed in $M_i=1.8$ jet (figure 5).

Parameter	Upstream of Mach disk	Downstream
Mach No. (M)	3.25	0.46
Static pressure (p)	10.8 KPa	496 KPa

Density (ρ)	0.4 kg/m ³	1.63 kg/m ³
Refractive index (n)	1.00009	1.00037
Shock thickness: between 0.37 μ m and 0.62 μ m		
Laser Wavelength: 0.514 μ m		

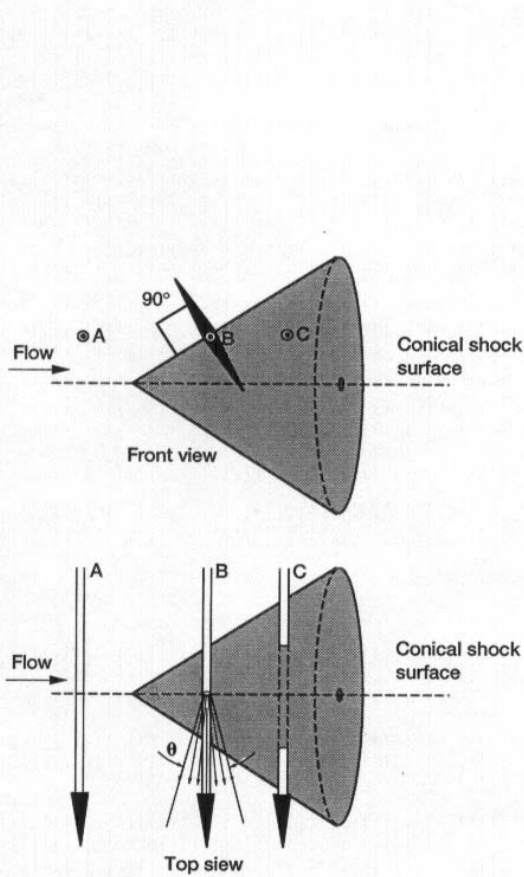


Figure 1.—Schematic of the optical phenomenon. A, B, and C are different positions of the laser beam which is normal to the plane of the paper in the front view and parallel in the top view.

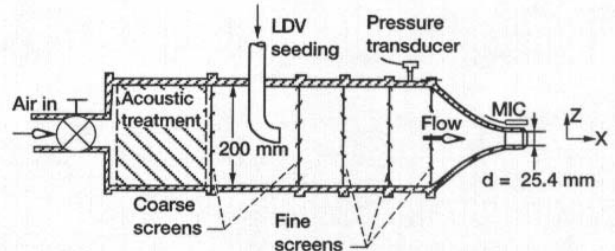


Figure 2.—Sketch of the free jet facility.

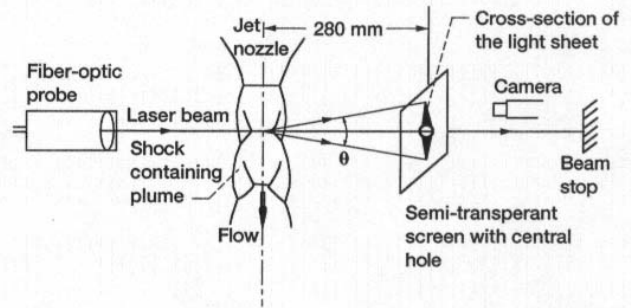
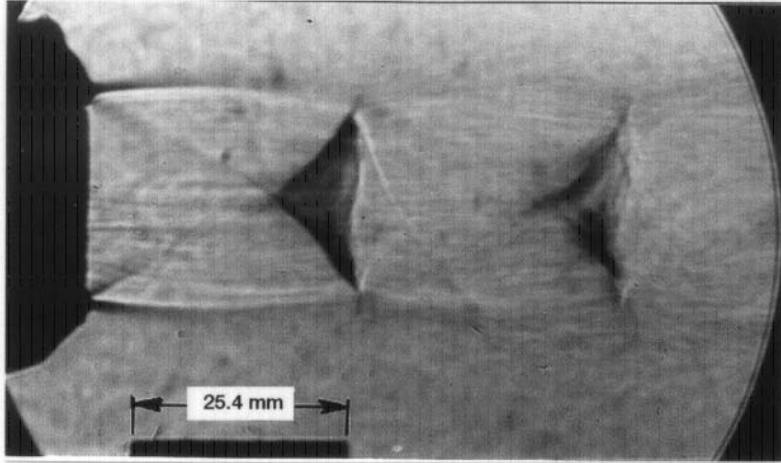
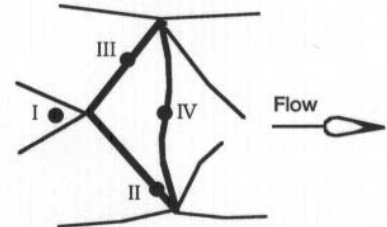


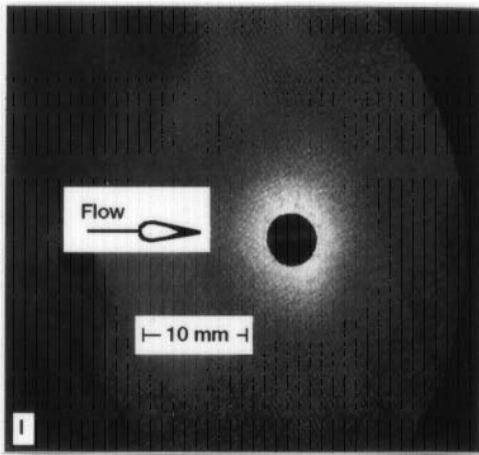
Figure 3.—Schematic of the arrangement to photograph a cross-section of the light sheet. The screen is parallel to the jet axis.



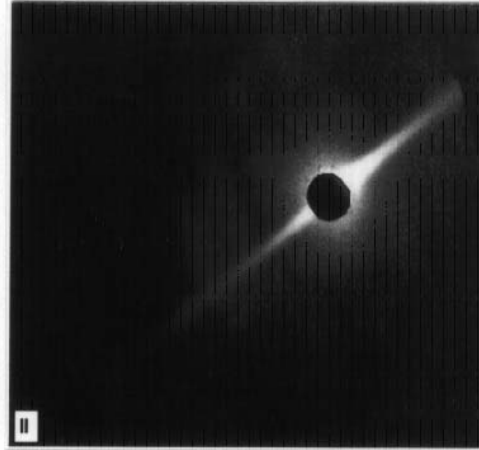
(a)



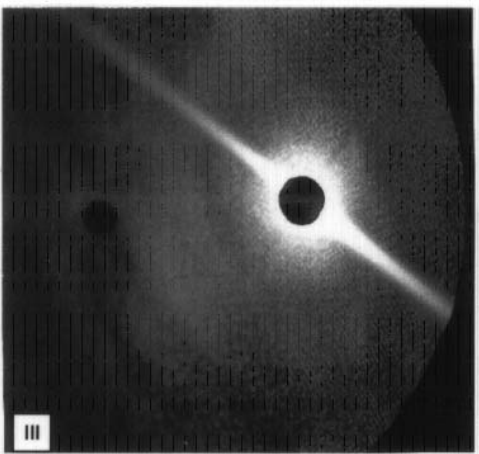
(b)



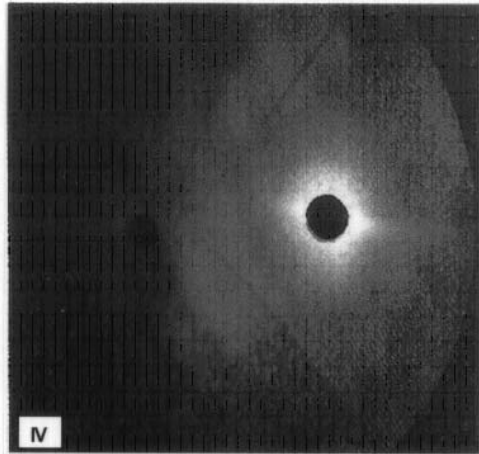
I



II



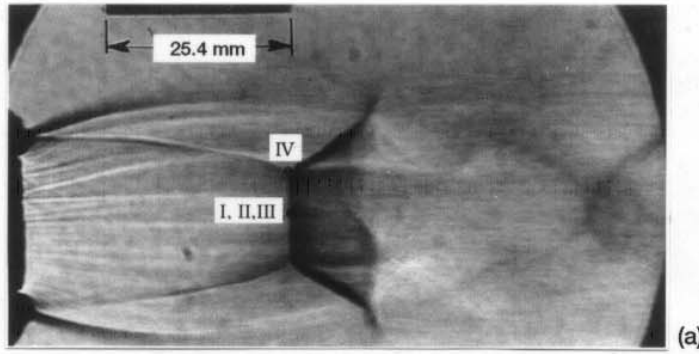
III



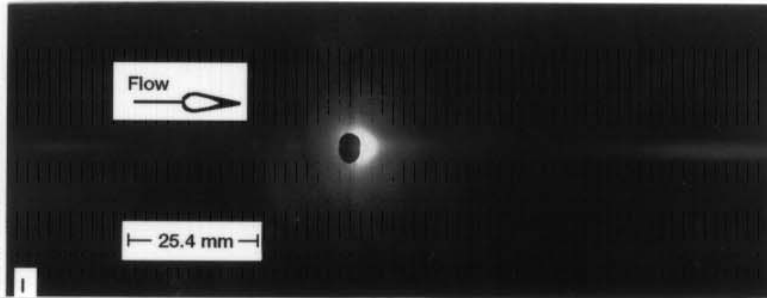
IV

(c)

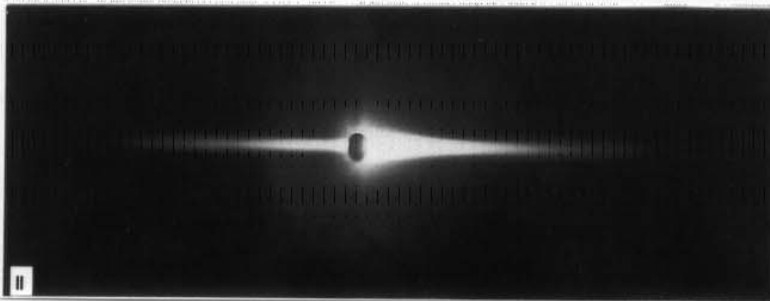
Figure 4.—Optical phenomenon as a laser beam crosses $M_1 = 1.4$ underexpanded jet. (a) Schlieren photograph, (b) Sketch of first shock cell and locations of the laser beam, (c) Cross-sectional views of the light sheet from indicated location.



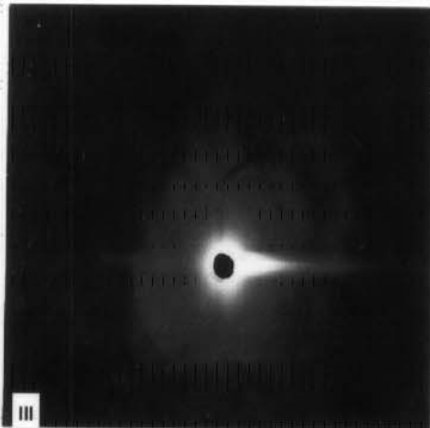
(a)



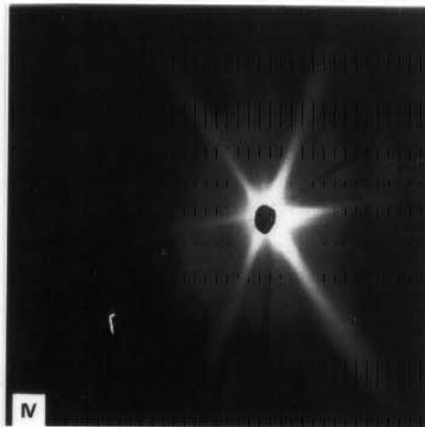
I



II



III



(b)

IV

Figure 5.—Optical phenomenon as a laser beam crosses $M_j = 1.8$ underexpanded jet. (a) Schlieren photograph and locations of the laser beam. Locations II and III are, respectively, 0.3 mm and 0.6 mm downstream from I. (b) Cross-sectional views of the light sheet from indicated locations.

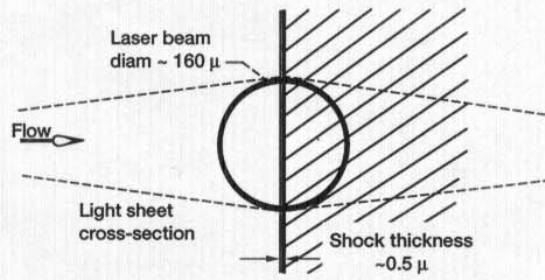


Figure 6.—Schematic of the shock-laser interaction at grazing incidence. The laser beam is normal to the plane of the paper.

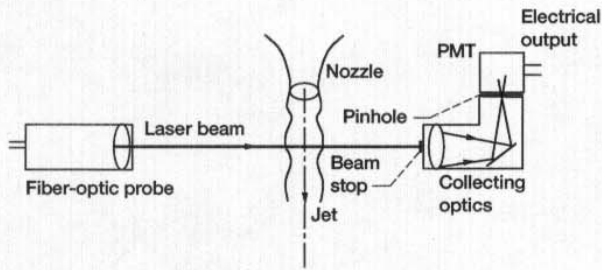


Figure 7.—Schematic of the shock detection technique.

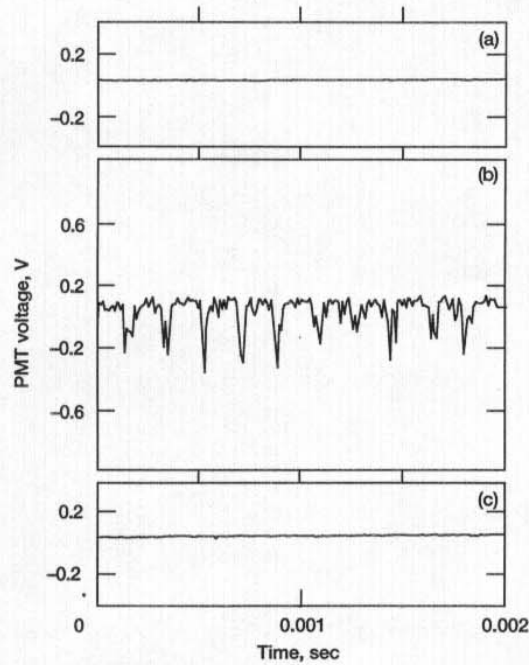


Figure 8.—PMT signals from the vicinity of the first shock surface of $M_j = 1.4$ jet; $z/D = 0.0$. (a) Just before shock. (b) Grazing the shock. (c) Piercing the shock.

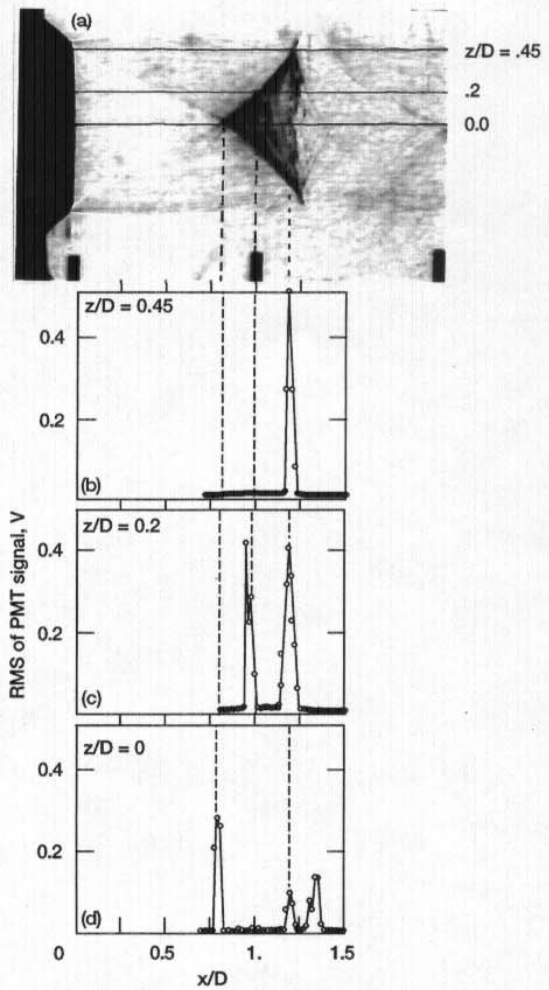


Figure 9.—Validation of the shock detection technique. (a) Schlieren photograph of the first shock surface in $M_j = 1.4$ jet. (b), (c) and (d) laser surveys at indicated radial positions.

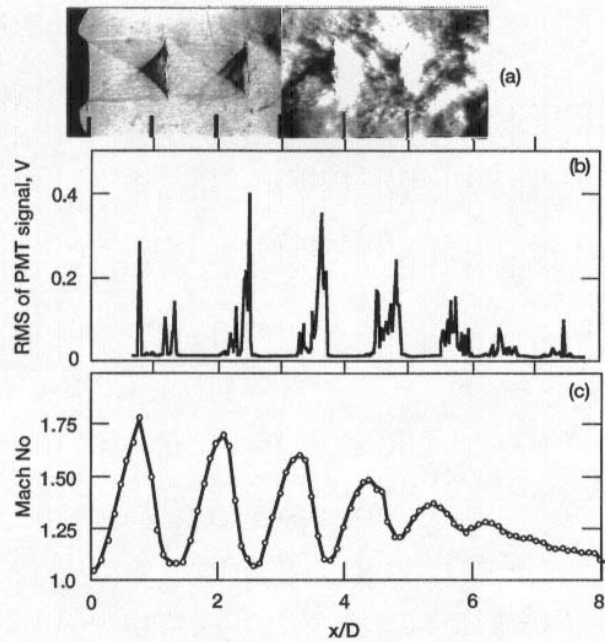


Figure 10.—Validation of the shock detection technique in $M_j = 1.4$ jet. (a) Spark schlieren photograph. (b) Laser survey along jet centerline. (c) LDV measurements of centerline axial velocity variation.

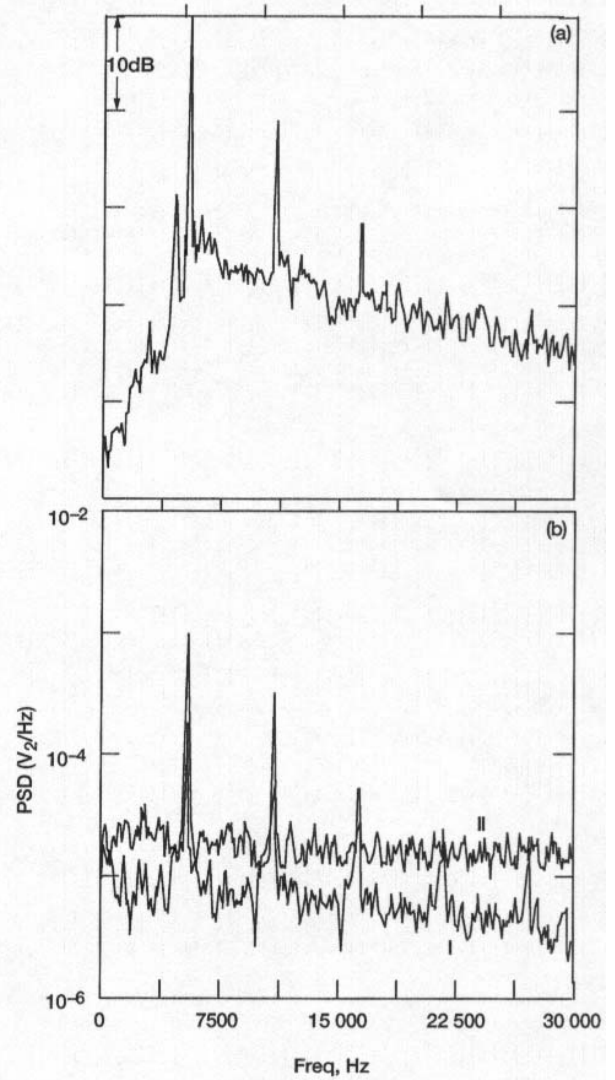


Figure 11.—Comparison between sound spectrum and shock unsteadiness in $M_j = 1.4$ jet. (a) Nearfield sound spectrum from nozzle lip. (b) Spectra of the PMT signal from indicated shocks, $z/D = 0.15$.